

# A tunable mixed feedback oscillator

Weiming Che, Fulvio Forni

**Abstract**—The interplay of positive and negative feedback loops on different time scales appears to be a fundamental mechanism for robust and tunable oscillations in both biological systems and electro-mechanical systems. We develop a detailed analysis of a basic three dimensional Lure model to show how controlled oscillations arise from the tuning of positive and negative feedback strengths. Our analysis is based on dominance theory and confirms, from a system-theoretic perspective, that the mixed feedback is a fundamental enabler of robust oscillations. Our results are not limited to three dimensional systems and extend to larger systems via passivity theory, and to uncertain systems via small gain arguments.

## I. INTRODUCTION

Oscillations are central in biology and engineering. In biology, oscillators appear in several biochemical processes [1], and play a crucial role in the sensory-information processing of neurons [2] and in rhythmic regulation in the body, such as breathing, chewing and walking [3]. In engineering, the interests in oscillators dates back to the 19th century, with the development of oscillating electrical circuits to support applications like digital clock generators and audio/video broadcast [4], [5]. More recent efforts in bio-inspired engineering aim at the design of tunable and resilient artificial oscillators for gait control in robotics [6], [7] and for neuromorphic circuits [8]. In spite of the substantial literature on the topic, the generation of self-excited oscillations in complex systems and the analysis of their stability/robustness features remain challenging questions [9].

The presence of both positive and negative feedback loops appears to be a recurrent structure in various biological oscillations [10]–[12]. Through dynamic conductances, neurons are extremely effective at combining positive and negative feedback, at several time scales, to achieve robust behavior and modulation capabilities in an uncertain setting [13]–[15]. This is confirmed by the engineering design of electrical oscillators, where the combination of positive and negative feedback pervades the early development of electrical amplifiers [4], [16], and is at the core of classical relaxation oscillator circuits [5], [17].

The challenge is to achieve robust oscillations in spite of unreliable components and dynamical uncertainties. Positive feedback increases the system sensitivity to input variations, leading to hysteresis, while negative feedback reduces this sensitivity, linearizing/normalizing the closed-loop behavior. Oscillations emerge from the interaction of these two feedback loops on different time scales [15]. The combination of fast positive feedback and slow negative feedback generates

a non-minimal zero in open loop, which becomes a source of instability in closed loop that leads to robust controlled oscillations. The aim of this paper is to develop a system theoretic analysis of this important phenomena.

Our analysis takes advantage of dominance theory and differential dissipativity [18], [19], rooted in the theory of monotone systems with respect to high rank cones [20]–[23]. Dominance theory allows us to identify/enforce a low dimensional “dominant” behavior (i.e. oscillations) in systems of any dimension, overcoming the usual restrictions to planar dynamics of Poincaré-Bendixson theory. It also allows us to analyze cases where describing function analysis shows limitations, typically due to dynamics that are not well represented by low harmonic approximations. Differential dissipativity provides instead the framework to tackle interconnections.

We study the effects of combined positive and negative feedback in the simple setting of Lure system modeling. In its simplest form, the controller is given by the parallel interconnection of two stable first order linear networks, one acting with positive sign and the other with negative sign. The positive branch is faster than the negative branch. Their relative strength is regulated by a *balance* parameter  $\beta$  while their collective strength is regulated by a *gain* parameter  $k$ . The controller acts on the plant, another stable first order linear network, through a simple sigmoidal saturation. The saturation is the only nonlinear element in our analysis. We close the loop by feeding back the output of the plant to the controller, as summarized in Fig. 1. We call this closed loop *mixed feedback amplifier*, to emphasize the crucial interplay of positive and negative feedback in determining the system behavior.

In what follows we take advantage of root locus analysis and Nyquist analysis, adapted to dominance theory, to derive sufficient conditions for controlled oscillations. We show how the closed loop behavior can be modulated from a stable equilibrium into stable oscillations by tuning the balance and the gain of the feedback. Taking inspiration from conductance-based models in neuroscience, we then generalize the analysis to controllers based on several parallel feedback lines (positive and negative). We also derive results for feedback interconnections, based on passivity, and we briefly touch upon the important topic of robustness to dynamic uncertainties.

The paper is organized as follows. Section II presents the main model equations. Section III is a brief introduction to dominance theory. Section IV shows the connection between the feedback parameters and the dominance properties of the closed loop. Section V completes the design of the feedback

W. Che is supported by CSC Cambridge Scholarship. W. Che and F. Forni are with the Department of Engineering, University of Cambridge, CB2 1PZ, UK [wc289|f.forni@eng.cam.ac.uk](mailto:wc289|f.forni@eng.cam.ac.uk)

parameters for oscillations. Extensions and interconnections are discussed in Section VI. Conclusion follows. The proofs of the theorems can be found in the arXiv version [24].

## II. THE MIXED FEEDBACK AMPLIFIER

We propose a simple mixed feedback amplifier model adapted from [14, Section III.C] and from the recently proposed neuromorphic circuit model [8], which shows how oscillations can be shaped via system parameter tuning.

The mixed feedback amplifier consists of three parts: a load associated with state variable  $x$  mimicking the passive membrane of a neuron, combined with positive feedback with state variable  $x_p$ , and negative feedback with state variable  $x_n$ . The feedback signals are summed and fed into a static sigmoidal saturation nonlinearity before closing the loop as shown in Fig. 1. Load, positive, and negative networks are simple first-order lags, a constraint that we will relax later in the paper. The resulting amplifier is represented by the differential equations

$$\begin{cases} \tau_l \dot{x} &= -x + u \\ \tau_p \dot{x}_p &= x - x_p \\ \tau_n \dot{x}_n &= x - x_n \\ u &= -\varphi(y) + r \\ y &= k(-\beta x_p + (1 - \beta)x_n) \end{cases} \quad (1)$$

where  $\tau_l, \tau_p, \tau_n$  are time constants of load, positive, and negative feedback networks respectively;  $r$  is the external input, typically held constant. The Lure structure of the closed loop is emphasized by the selection of the load input  $u$  and of the mixed feedback output  $y$ . The mixed feedback is characterized by two main parameters, the *gain*  $k \geq 0$  and the *balance*  $0 \leq \beta \leq 1$ , the latter capturing the relative strength between positive and negative feedback.

The transfer functions of load, positive, and negative networks respectively read

$$L(s) = \frac{1}{\tau_l s + 1}, \quad Cp(s) = \frac{1}{\tau_p s + 1}, \quad Cn(s) = \frac{1}{\tau_n s + 1}. \quad (2)$$

Each network is associated with a pole  $p_l = -\frac{1}{\tau_l}$ ,  $p_p = -\frac{1}{\tau_p}$  and  $p_n = -\frac{1}{\tau_n}$ . We assume a well-defined time scale separation,

$$\tau_p < \tau_n, \quad (3)$$

between the positive and negative feedback networks. For simplicity of the exposition, we assume that the time constant  $\tau_l$  is never equal to  $\tau_p$  or  $\tau_n$ . We also assume that  $\varphi$  is slope-restricted, differentiable function

$$0 \leq \varphi' \leq 1 \quad (4)$$

and such that  $\varphi'(y) = 0$  whenever  $|y|$  is larger than a given threshold  $M$  ( $M$  can be any). For simplicity, simulations will use  $\varphi = \tanh$ .

We look at (1) as a Lure system, which is the negative feedback interconnection of the transfer function from input  $u$  to output  $y$  given by

$$G(s, k, \beta) = \frac{-k((\beta(\tau_n + \tau_p) - \tau_p)s + 2\beta - 1)}{(\tau_l s + 1)(\tau_p s + 1)(\tau_n s + 1)} \quad (5)$$

and the sigmoidal nonlinearity  $\varphi$ . This allows us to examine the effects of variations in the mixed feedback gain and balance by using classical linear tools, like root locus analysis, Nyquist diagrams, and a generalized circle criterion adapted to the recently developed dominance theory [18], [19].

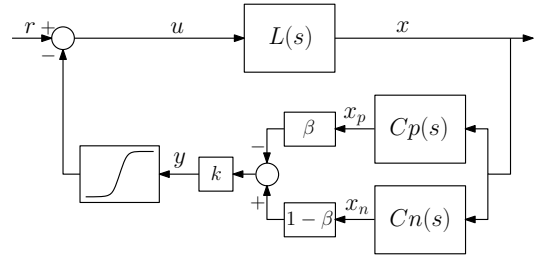


Fig. 1. Block diagram of the mixed feedback amplifier.

## III. DOMINANCE THEORY

Dominance theory aims to capture the existence of low dimensional attractors in a high dimensional system state space. For linear system  $\dot{x} = Ax$ ,  $x \in \mathbb{R}^n$ ,  $p$ -dominance means that the dynamics can be split into  $p$  slow dominant modes and  $n - p$  fast transient modes. For nonlinear systems

$$\dot{x} = f(x), \quad x \in \mathbb{R}^n \quad (6)$$

dominance can be characterized by using the linearization along the system trajectories (capturing infinitesimal variations in the neighborhood a generic trajectory  $x(\cdot)$ )

$$\begin{cases} \dot{x} = f(x) \\ \delta \dot{x} = \partial f(x) \delta x \end{cases} \quad (x, \delta x) \in \mathbb{R}^n \times \mathbb{R}^n. \quad (7)$$

*Definition 1:* The nonlinear system (6) is  $p$ -dominant with rate  $\lambda \geq 0$  if and only if there exist a symmetric matrix  $P$  with inertia  $(p, 0, n - p)$  and  $\varepsilon \geq 0$  such that (7) satisfies the conic constraint

$$\begin{bmatrix} \delta \dot{x} \\ \delta x \end{bmatrix}^T \begin{bmatrix} 0 & P \\ P & 2\lambda P + \varepsilon I \end{bmatrix} \begin{bmatrix} \delta \dot{x} \\ \delta x \end{bmatrix} \leq 0 \quad (8)$$

along all its trajectories. The property is strict if  $\varepsilon > 0$ . Here the symmetric matrix  $P$  with inertia  $(p, 0, n - p)$  has  $n - p$  positive eigenvalues and  $p$  negative eigenvalues;  $p$  is the dimension of the dominant sub-dynamics of the nonlinear system. We are particularly interested in small  $p$  as this entails that the nonlinear system possesses a simple attractor, as summarized in the next theorem, [18, Corollary 1].

*Theorem 1:* For a strict  $p$ -dominant system (6) with dominant rate  $\lambda \geq 0$ , every bounded trajectory asymptotically converges to

- a unique fixed point if  $p = 0$ ;
- a fixed point if  $p = 1$ ;
- a simple attractor if  $p = 2$ , that is, a fixed point, a set of fixed points and connecting arcs, or a limit cycle.

For the analysis of the mixed feedback amplifier we are particularly interested in the case  $p = 2$ , where the asymptotic behavior of the system is essentially captured by a planar

system. As a result, we can predict the existence of the stable oscillations if all equilibrium points of the system are unstable and trajectories remain bounded.

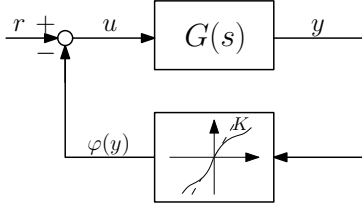


Fig. 2. Lure feedback system

For Lure feedback systems,  $p$ -dominance can be also characterized in the frequency domain, through the circle criteria for  $p$ -dominance, [19, Corollary 4.5].

*Theorem 2 (Circle criteria for  $p$ -dominance):* Consider the Lure feedback system in Fig. 2 given by the negative feedback interconnection of the linear system  $G(s)$  and the static nonlinearity  $\varphi$  satisfying sector condition  $\partial\varphi \in (0, K)$ . The closed system is strictly  $p$ -dominant with rate  $\lambda$  if:

- 1) the real parts of all the poles of  $G(s)$  not equal to  $-\lambda$ ;
- 2) the shifted transfer function  $G(s - \lambda)$  has  $p$  unstable poles;
- 3) the Nyquist plot of  $G(s - \lambda)$  lies to the right hand side of the line  $-1/K$  on the Nyquist plane.  $\lrcorner$

Theorem 2 will be extensively used in this paper. It will be particularly useful when combined to the notion of  $p$ -passivity, [18]. Indeed, a linear system with transfer function  $G(s)$  is  $p$ -passive with rate  $\lambda$  if it satisfies the conditions of Theorem 2 for  $K = \infty$ . In such a case, the Lure system in Fig. 2 is also  $p$ -passive from  $r$  to  $y$ , [19]. Thus, a  $p$ -passive system is a  $p$ -dominant system. Furthermore,  $p$ -passivity is preserved by negative feedback interconnections, as clarified by the following theorem, [18].

*Theorem 3:* Consider two systems  $\Sigma_i$  and assume they are respectively  $p_i$ -passive with common rate  $\lambda$  with input  $u_i$  and output  $y_i$ , where  $i \in \{1, 2\}$ . Then, the negative feedback loop given by  $u_1 = -y_2 + r_1$  and  $u_2 = y_1 + r_2$  is  $(p_1 + p_2)$ -passive from  $(r_1, r_2)$  to  $(y_1, y_2)$ .

#### IV. FEEDBACK TUNING VIA DOMINANCE THEORY

The linear system  $G(s, k, \beta)$  in (5) is stable with poles in  $-\frac{1}{\tau_i}$ ,  $-\frac{1}{\tau_p}$ , and  $-\frac{1}{\tau_n}$ . Once the time constants are fixed, the system's behavior is modulated by the balance  $\beta$  and by the gain  $k$ .  $\beta$  determines the position of the zero of  $G(s, k, \beta)$ ,

$$z = \frac{2\beta - 1}{\beta(\tau_p + \tau_n) - \tau_p}. \quad (9)$$

The zero has positive real part for  $\beta > 0.5$ , i.e. when the contribution of the positive feedback component is sufficiently strong. Combined with a large gain  $k$ , looking at the root locus of the linearized closed loop, the zero acts as an ‘‘attractor’’ for the closed-loop poles, to guarantee (a controlled) instability of the unsaturated closed loop equilibrium (for  $r = 0$ ). This zero and its modulation via  $\beta$  is the fingerprint of the mixed feedback amplifier. It

guarantees robust modulation between the stable regime and the unstable/oscillatory regime of the closed-loop system.

For all  $\beta \in [0, 1]$ ,  $G(s, k, \beta)$  is a stable transfer function therefore the closed loop remains stable for sufficiently small gain  $k$ , as certified by the following theorem.

*Theorem 4:* For any constant  $r$  and any  $\beta \in [0, 1]$ , the system (1) is 0-dominant with  $\lambda = 0$  for any gain  $0 \leq k < \bar{k}_0$  given by

$$\bar{k}_0 = \begin{cases} \infty & \text{if } \min_{\omega} \Re(G(j\omega, 1, \beta)) \geq 0 \\ -\frac{1}{\min_{\omega} \Re(G(j\omega, 1, \beta))} & \text{otherwise.} \end{cases} \quad (10)$$

Using the circle criterion, the closed system is 0-dominant as long as the Nyquist plot of (5) remains to the right of the shaded region in Fig. 3. Given the boundedness of  $|G(s, 1, \beta)|_{\infty}$ , the exact value of  $\bar{k}_0$  can be determined numerically as in (10).  $\lrcorner$

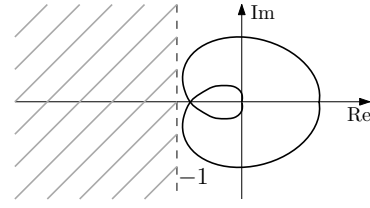


Fig. 3. An illustration of the proof of 0-dominance using circle criteria. The shaded region denotes the constraint to the Nyquist plot of  $G(s, k, \beta)$ , set by nonlinearity  $\varphi$ . The Nyquist locus represents the case of a zero in (9) has positive real part.

We now look into the tuning of  $k$  and  $\beta$  to enable oscillations, using the shifted transfer function  $G(s - \lambda, k, \beta)$  and focusing on 2-dominance. As first step, the rate  $\lambda$  must be chosen to ensure that  $G(s - \lambda, k, \beta)$  has two unstable poles, a necessary condition for dominance due to specific (differential) sector condition  $0 \leq \varphi' \leq 1$ .

*Theorem 5:* Consider a rate  $\lambda$  for which the transfer function  $G(s - \lambda, k, \beta)$  has two unstable poles. Then, for any constant  $r$  and any  $\beta \in [0, 1]$ , the system (1) is 2-dominant with rate  $\lambda$  for any gain  $0 \leq k < \bar{k}_2$  given by

$$\bar{k}_2 = \begin{cases} \infty & \text{if } \min_{\omega} \Re(G(j\omega - \lambda, 1, \beta)) \geq 0 \\ -\frac{1}{\min_{\omega} \Re(G(j\omega - \lambda, 1, \beta))} & \text{otherwise.} \end{cases} \quad (11)$$

The proof argument simply follows the one of Theorem 4 applied to the shifted transfer function.

Theorem 4 and 5 show that there is a range of gains  $k$  for which the system is at the same time 0-dominant and 2-dominant. This is not a contradiction, since the range of behaviors of a 0-dominant system is compatible with the range of behaviors of a 2-dominant system. The system behavior will be constrained by the most restrictive of the two properties, namely 0-dominance, ensuring that all trajectories converge to a unique equilibrium. As a result, in tuning parameters for oscillations, we will explore the range of gains  $\bar{k}_0 < k < \bar{k}_2$ .

When the positive feedback is strong enough the close system (1) becomes 2-passive, as clarified below.

**Theorem 6:** Consider the critical balance  $\beta^* = \frac{\tau_p}{\tau_p + \tau_n}$ . For any  $\beta \in (\beta^*, 1]$ , there exist a rate  $\lambda \geq 0$  for which the system (1) is 2-passive from  $r$  to  $y$ , for any  $k \geq 0$ .  $\square$

For a suitable selection of  $\lambda$  and  $\beta \in (\beta^*, 1]$ , Theorem 6 guarantees that  $\bar{k}_2 = \infty$  (in Theorem 5). We also observe that the critical balance  $\beta^*$  tends towards zero as the positive feedback component becomes faster, i.e.  $\tau_p \rightarrow 0$ . Finally, taking advantage of Theorem 3, 2-passivity of (1) means that we can interconnect the mixed feedback amplifier with other 0-passive systems while preserving 2-passivity.

## V. FEEDBACK CONTROL OF OSCILLATIONS

Based on the analysis in section IV, the parametric range for the mixed feedback amplifier to be 0-dominant, 2-dominant, and 2-passive can be derived numerically for any given set of the time constants  $\tau_l$ ,  $\tau_p$ ,  $\tau_n$  that satisfy the key assumption of time scale separation between positive and negative feedbacks. Oscillations will arise for gains  $\bar{k}_0 < k < \bar{k}_2$ , when the system is 2-dominant but not 0-dominant, as typically identified by the presence of (at least) one unstable equilibrium in closed loop. The existence of this unstable equilibrium is guaranteed by the attraction exerted on the closed loop poles by the unstable zero (9), for a suitable selection of  $\beta$  and for a sufficiently large gain  $k$ . In fact, the stability of the open-loop transfer function  $G(s, k, \beta)$  combined with the conditions on  $\varphi$  guarantee that the trajectories of the closed-loop system are bounded for any balance  $\beta \in [0, 1]$  and gain  $k \geq 0$ . Therefore, by Theorem 1, oscillations will arise when the closed loop is 2-dominant and has only unstable equilibria. When some of the equilibria are stable, oscillations may coexist with them.

The number of equilibria of the closed loop can be determined by looking at the intersection of the static nonlinearity  $\varphi(y)$  (here we use  $\varphi = \tanh$ ) with the line  $\frac{y}{k(2\beta-1)}$ , where

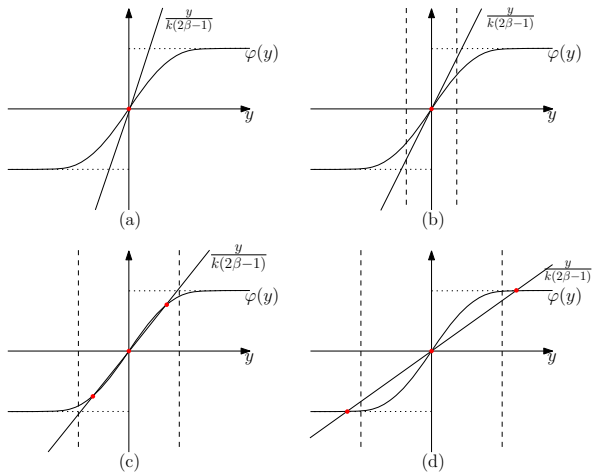


Fig. 4. Four situations of the stability of the equilibrium points for  $\beta \in (0.5, 1)$ , input  $r = 0$ . The fixed points are unstable if it falls in the region bounded by the dashed lines. The case  $r \neq 0$  is similar, taking into account a vertical shift to  $\varphi(y)$ .

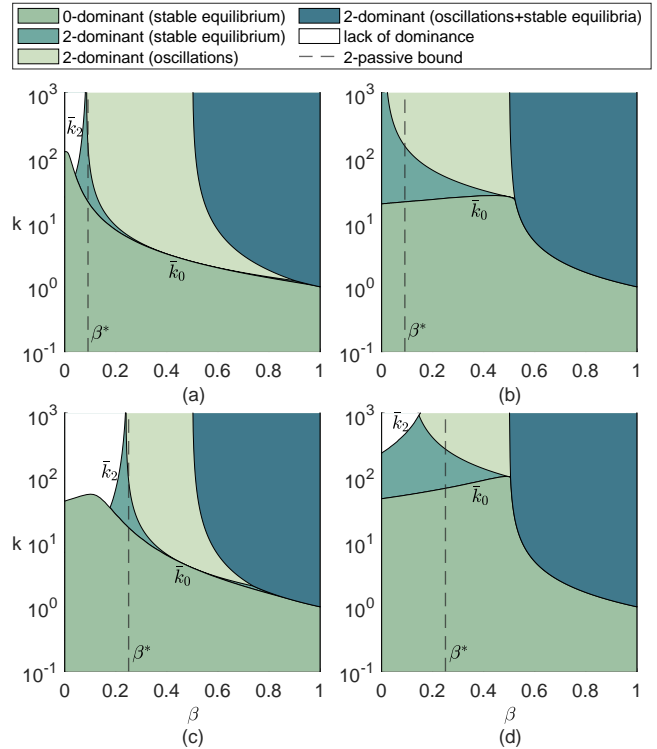


Fig. 5. Dominance map for input  $r = 0$ . (a) fast load:  $\tau_l = 0.01$ ,  $\tau_p = 0.1$ ,  $\tau_n = 1$ ,  $\lambda = 50$ ; (b) slow load:  $\tau_l = 10$ ,  $\tau_p = 0.1$ ,  $\tau_n = 1$ ,  $\lambda = 5$ ; (c) fast load, reduced time-scale separation:  $\tau_l = 0.01$ ,  $\tau_p = 0.1$ ,  $\tau_n = 0.3$ ,  $\lambda = 50$ ; (d) slow load, reduced time-scale separation:  $\tau_l = 10$ ,  $\tau_p = 0.1$ ,  $\tau_n = 0.3$ ,  $\lambda = 5$ .

$k(2\beta - 1)$  is the DC gain of  $G(s, k, \beta)$  (5). For  $\varphi = \tanh$ , when  $\beta \in [0, 0.5]$ , we have that  $k(2\beta - 1) < 0$  therefore we have one equilibrium in zero. The equilibrium is stable if  $k$  is smaller than the gain margin of  $G(s, 1, \beta)$ . When  $\beta \in (0.5, 1]$ , for small  $k$  in Fig. 4a, the lack of dashed lines shows that the equilibrium is stable and there are no oscillations. As  $k$  and  $\beta$  increases, the 0 equilibrium becomes unstable and oscillations appear, Fig. 4b. For larger values, two (and more) unstable equilibria emerge, preserving oscillations, Fig. 4c. They eventually become stable, and oscillations may disappear or coexist with stable equilibria, Fig. 4d. Exact gain  $k$  and balance  $\beta$  at which such stability change takes place can be determined numerically.

For illustration, we fix the reference  $r = 0$  and we derive four parametric maps on the dominance of the mixed feedback amplifier for  $k \in (0.1, 1000)$  and  $\beta \in [0, 1]$ , for different time scale arrangements, as shown in Fig. 5. Here, for simplicity, we set  $\lambda$  roughly in the middle of the leftmost pair of poles (this guarantees the additional property of 2-passivity).

Moving horizontally on Fig. 5, we see that increase in  $\beta$  modulates the closed-loop behavior from global stability of an equilibrium into oscillations (eventually leading to multi-stability), for  $k$  within a suitable range. Likewise, moving vertically on Fig. 5, we see that oscillations are always triggered (dampened) by increasing (decreasing) the feedback gain  $k$ , for  $\beta$  within a suitable range. Fig. 5

also shows numerically how a larger time scale separation guarantees a larger region of oscillations and a lower critical balance  $\beta^*$  for 2-passivity.

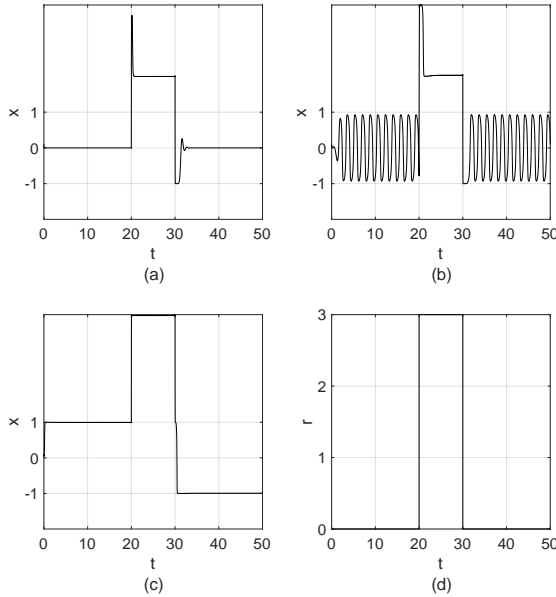


Fig. 6. Simulations of the mixed-feedback amplifier in response to the input reference  $r$ , from the initial condition  $x = 0.1$ ,  $x_p = 0$  and  $x_n = 0$ , and different tuning of  $k$  and  $\beta$ . (a):  $k = 5$ ,  $\beta = 0.2$  (0-dominant); (b):  $k = 5$ ,  $\beta = 0.4$  (2-dominant, oscillation); (c):  $k = 5$ ,  $\beta = 0.8$  (2-dominant oscillation + stable equilibria).

We complete our discussion with simulations, in Fig. 6. We consider time constants as in Fig. 5a and we select gain and balance to explore the three main regions in the figure: 0-dominance is illustrated in Fig. 6a, 2-dominance (oscillations) is in Fig. 6b, and the last case of 2-dominance (oscillations + stable equilibria) is in Fig. 6c. Fig. 6d illustrates the piecewise constant input  $r$  used to perturb the system from its steady state for  $20 \leq t \leq 30$  (bottom right). After the step change in the reference  $r$ , the state trajectories of the system tuned in the 0-dominant region, Fig. 6a, and in the 2-dominant (oscillation) region, Fig. 6b, converge back to the original steady state. For the system tuned in the 2-dominant (oscillations + stable equilibria) region, Fig. 6c, the trajectory starts from one of the stable equilibria and, after reference perturbation, converges to the other one.

## VI. LARGE MIXED FEEDBACK SYSTEMS

### A. Multi-channel mixed feedback amplifier

The results presented in the previous sections can be extended to larger systems. As first example, in this section we take inspiration from neuroscience, where the membrane electrical potential of a neuron is modulated by multiple parallel ion channels [13], [14], [25]. Thus, we show how the mixed feedback structure can be extended to a larger parallel of first order systems while preserving the overall closed-loop behavior and modulation features. In fact, looking at Fig. 1, for a slow first order  $L(s)$  and for  $Cp(s)$  and  $Cn(s)$  given by the sum of several first order networks with similar

time scales,  $\sum_i \frac{1}{\tau_i s - 1}$ , the resulting system shows clustered and interlaced poles and zeros, which have negligible effects on the dominance properties to the system.

*Proposition 1:* Let  $C(s)$  be the difference of two finite parallels of first order transfer functions separated by a well-defined time scale:

$$\begin{aligned} C(s) &= \beta Cp(s) - (1 - \beta)Cn(s) \\ &= \beta \sum_{i=1}^m \frac{\rho_i}{\tau_i s + 1} - (1 - \beta) \sum_{i=m+1}^{m+n} \frac{\rho_i}{\tau_i s + 1}, \end{aligned} \quad (12)$$

where

$$-\frac{1}{\tau_1} < -\frac{1}{\tau_2} < \dots < -\frac{1}{\tau_m} < -\frac{1}{\tau_{m+1}} < \dots < -\frac{1}{\tau_{m+n}}$$

and  $\sum_{i=1}^m \rho_i = 1$  and  $\sum_{i=m+1}^{m+n} \rho_i = 1$  (unit gain). Then for  $\beta \in (0, 1)$ ,

- the poles of  $C(s)$  are those of  $Cp(s)$  and  $Cn(s)$ .
- $C(s)$  has  $m + n - 1$  zeros, where
  - $m - 1$  zeros are interlaced with the poles of  $Cp(s)$  on real axis;
  - $n - 1$  zeros are interlaced with the poles of  $Cn(s)$  on real axis;
  - one zero lies on the real axis and locates in  $(-\infty, -1/\tau_1) \cup (-1/\tau_{m+n}, \infty)$ .

Proposition 1 makes straightforward to generalize dominance analysis to the high dimensional mixed feedback amplifier. The extended open-loop transfer function  $\bar{G}(s, k, \beta)$  has the structure

$$\bar{G}(s, k, \beta) = G(s, k, \beta)G_e(s) \quad (13)$$

where  $G(s, k, \beta)$  corresponds to (5), with a fast pole  $p_p$ , two slow poles  $p_n$  and  $p_l$  and a right-most zero  $z$  (for sufficiently large  $\beta$ ), and  $G_e(s)$  is a bi-proper transfer function collecting the remaining poles and zeros, as shown in Fig. 7).

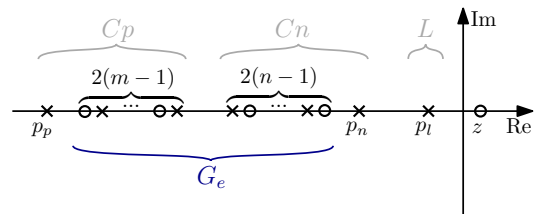


Fig. 7. An illustration of pole-zero distribution of  $\bar{G}(s, k, \beta)$ .

Under the assumptions of Proposition 1, it is straightforward to show that Theorems 4 and 5 hold for the Lure system given by  $\bar{G}(s, k, \beta)$  and  $\varphi$  (using the same proof argument). Furthermore, in spite of the extended system dimension, the number and stability of the closed-loop equilibria can be analyzed as in Section V, looking at the intersection between  $\varphi$  and the line with slope given by  $\bar{G}(j\omega, k, \beta)$ , and to the root locus of  $\bar{G}(s, k, \beta)$ . Thus, through the root locus, their stability is fundamentally related to the relative degree of  $\bar{G}(s, k, \beta)$  combined to the presence of an unstable right-most zero ( $z$  in figure 7). This means that Fig. 4 holds thus, for sufficiently large  $\beta$  and  $k$ , the system will oscillate as

the consequence of 2-dominance combined with unstable equilibria.

### B. Passive external loads

Theorem 6 shows that the mixed feedback amplifier (1) is 2-passive from  $r$  to  $y$  for a suitable selection of balance  $\beta$  and gain  $k$ . Thus, by Theorem 3, feedback interconnections with any 0-passive system (sharing the same rate  $\lambda$ ) will preserve 2-passivity, i.e. 2-dominance. This suggests a route to build larger 2-passive systems through interconnection, as shown in Fig. 8. It also illustrates the role of the mixed feedback amplifier as a feedback controller driving stable 0-passive loads into oscillations.

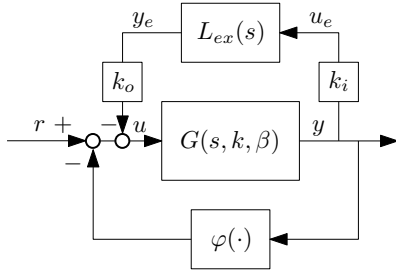


Fig. 8. The interconnection of load and the mixed feedback amplifier

We consider here a linear load  $L_{ex}(s)$ , modeling a generic mass-spring-damper system. The interface between mixed feedback amplifier and external load is represented by simple linear coefficients  $k_o > 0$  and  $k_i > 0$ , as shown in in Fig. 8. The mass-spring-damper system transfer function from the force input  $u_e$  to the mixed velocity/position output  $y_e$  reads

$$L_{ex}(s) = \frac{k_v s + k_p}{s^2 + b s + a} \quad (14)$$

where  $b > 0$  and  $a > 0$  are normalized damping coefficient and spring constant, respectively. The output is a weighted combination of velocity and position variables, through the gains  $k_v > 0$  and  $k_p > 0$ .

To build a 2-passive interconnection, we need to show 0-passivity of the the mass-spring-damper system for a given rate  $\lambda \geq 0$ . For the sake of illustration, consider  $b = 35$  and  $a = 350$  which give stable poles with real part smaller than  $-\lambda$ , for  $\lambda = 15$ . For these parameters,  $L_{ex}(s)$  is 0-passive for  $k_v = 1$  and  $k_p = 20$ , which guarantee that  $L_{ex}(s - \lambda)$  is positive real as illustrated by the Nyquist plot in Fig. 9 (left). Note that, differently from the case  $\lambda = 0$ , velocity feedback is not enough to guarantee 0-passivity for  $\lambda > 0$ . A combination of velocity and position feedback is required to enforce 0-passivity, through the phase contribution of a stable zero in the transfer function.

Given the parameters of the mass-spring-damper system, we consider a mixed feedback amplifier based on a fast internal load  $L(s)$  with time constant  $\tau_l = 0.01$  (negligible), and positive and negative feedback time constants  $\tau_p = 0.1$  and  $\tau_n = 1$ . The mixed feedback amplifier is tuned for 2-passivity with rate  $\lambda = 15$  by taking gain  $k = 10$  and balance  $\beta = 0.4$ , which also correspond to an oscillatory regime for  $r = 0$  for the mixed feedback amplifier in isolation.

From Theorem 3, the negative feedback interconnection of the mixed feedback amplifier with the mass-spring-damper system is 2-passive. Preserving 2-passivity does not guarantee that the feedback loop will continue to oscillate, since 2-passivity is also compatible with the presence of a stable equilibrium. However, if the overall closed-loop equilibria are unstable and trajectories are bounded, the closed-loop system will oscillate. In the example this is achieved by tuning the interconnection gains  $k_i$  and  $k_o$ . A stable oscillatory regime is obtained for  $k_o = 1$  and  $k_i = 10$ , as shown in Fig. 9 (right).

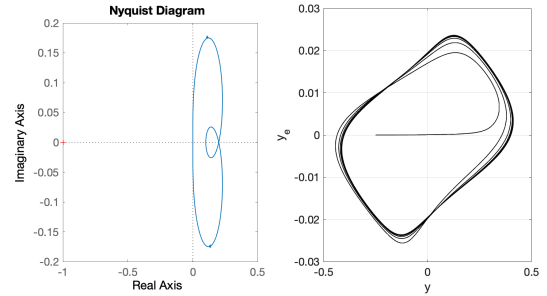


Fig. 9. Left: Shifted Nyquist plot of the mass-spring-damper system  $L_{ex}(s - \lambda)$ ;  $\lambda = 15$ ,  $k_v = 1$ ,  $k_p = 20$ ,  $d = 35$ ,  $k = 350$ ; Right: Trajectory of interconnected system projected on  $(y, y_e)$  plane, with  $\tau_l = 0.01$ ,  $\tau_p = 0.1$ ,  $\tau_n = 1$ ,  $k = 10$ ,  $\beta = 0.4$ ,  $k_i = 10$ ,  $k_o = 1$ .

*Remark 1:* In comparison to entrainment phenomena, which are typically identified by a cascade structure, these oscillations arise from the feedback interconnection of the mixed feedback amplifier with an external load. They are thus shaped by the respective features of the two systems. This means, for example, that oscillations may emerge from the interconnection of the mixed feedback amplifier with an external load even if the two systems in isolation do not oscillate.

### C. Robustness to unmodeled dynamics

We briefly touch upon the robustness properties of the mixed feedback amplifier, which can be discussed within the classical framework of robust control, using dynamic uncertainties  $\Delta_l$ ,  $\Delta_p$ ,  $\Delta_n$  as shown in Fig. 10.

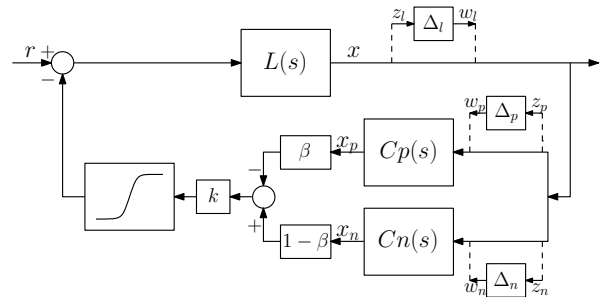


Fig. 10. The mixed feedback amplifier with multiplicative unmodeled dynamics  $\Delta_l$ ,  $\Delta_p$ , and  $\Delta_n$  associated with  $L(s)$ ,  $Cp(s)$ , and  $Cn(s)$ .

A qualitative perspective is provided by Theorem 2, which makes clear that small perturbations on the shape of the

Nyquist plot of the open-loop transfer function  $G(s, k, \beta)$  cannot change the  $p$ -dominance of the system. This simple graphical observation suggests that  $p$ -dominance is a robust property. For a quantitative perspective, the robustness of  $p$ -dominance property of the mixed-feedback amplifier can be studied using small-gain results, adapted to dominance through the notion of  $p$ -gain. Not surprisingly, the feedback interconnection of a  $p$ -dominant system with 0-dominant uncertainties  $\Delta_l$ ,  $\Delta_p$ , and  $\Delta_n$  remains  $p$ -dominant if the product of their gains is sufficiently small (their product must be less than one, as in the classical stability [18], [26]).

In summary, small 0-dominant perturbations with rate  $\lambda$ , will preserve the dominance properties of the mixed feedback amplifier. Moreover, the stability/instability of the closed-loop equilibria will also remain unchanged for sufficiently small perturbations. This means that the stable / oscillatory regimes of the mixed feedback are robust. A quantitative analysis can be developed through convex optimization, based on linear matrix inequalities [18], [26].

## VII. CONCLUSIONS

We use dominance analysis to achieve controlled robust oscillations in closed loop, by combining positive and negative feedback. The design is inspired by insightful observations from biology, neuroscience, and electronics, which identify in the mixed feedback a fundamental source of robust and tunable oscillations. We provide a system-theoretic analysis of the mixed feedback amplifier, within the simplified setting of Lure system modeling. Our analysis is based on dominance theory and shows how to tune feedback gain and feedback balance to control the closed-loop behavior. We later extend the analysis to larger systems. We study large parallels of positive and negative feedback, mimicking the structure of conductance-based models in neuroscience. We also tackle passive interconnections to control oscillations of interconnected loads. We finally discuss briefly the robustness of the mixed amplifier, a topic that will be developed in details in other publications. In fact, many directions are left to explore, starting from the problem of shaping the oscillation regime through feedback and the problem of feedback design for robustness. The problem of shaping the oscillation frequency of the mixed feedback amplifier is studied in the follow up paper [27].

## ACKNOWLEDGMENTS

The authors would like to thank Rodolphe Sepulchre for very insightful discussions on the mixed feedback amplifier and on conductance-based models in neuroscience. These have been very helpful to shape our paper.

## REFERENCES

- [1] A. Goldbeter, *Biochemical Oscillations and Cellular Rhythms: The Molecular Bases of Periodic and Chaotic Behaviour*. Cambridge University Press, 1997.
- [2] S. M. Sherman, "Tonic and burst firing: dual modes of thalamocortical relay," *Trends in neurosciences*, vol. 24, no. 2, pp. 122–126, 2001.
- [3] E. Marder and D. Bucher, "Central pattern generators and the control of rhythmic movements," *Current biology*, vol. 11, no. 23, pp. R986–R996, 2001.

- [4] D. Tucker, "The history of positive feedback: The oscillating audion, the regenerative receiver, and other applications up to around 1923," *Radio and Electronic Engineer*, vol. 42, no. 2, pp. 69–80, 1972.
- [5] J. Ginoux and C. Letellier, "Van der pol and the history of relaxation oscillations: Toward the emergence of a concept," *Chaos: An Interdisciplinary Journal of Nonlinear Science*, vol. 22, no. 2, p. 023120, 2012.
- [6] A. J. Ijspeert, A. Crespi, D. Ryczko, and J.-M. Cabelguen, "From swimming to walking with a salamander robot driven by a spinal cord model," *science*, vol. 315, no. 5817, pp. 1416–1420, 2007.
- [7] H. Kimura, S. Akiyama, and K. Sakurama, "Realization of dynamic walking and running of the quadruped using neural oscillator," *Autonomous robots*, vol. 7, no. 3, pp. 247–258, 1999.
- [8] L. Ribar and R. Sepulchre, "Neuromodulation of neuromorphic circuits," *IEEE Transactions on Circuits and Systems I: Regular Papers*, 2019.
- [9] A. J. Ijspeert, "Central pattern generators for locomotion control in animals and robots: a review," *Neural networks*, vol. 21, no. 4, pp. 642–653, 2008.
- [10] P. Smolen, D. A. Baxter, and J. H. Byrne, "Modeling circadian oscillations with interlocking positive and negative feedback loops," *Journal of Neuroscience*, vol. 21, no. 17, pp. 6644–6656, 2001.
- [11] A. Y. Mitrophanov and E. A. Groisman, "Positive feedback in cellular control systems," *Bioessays*, vol. 30, no. 6, pp. 542–555, 2008.
- [12] T. Y.-C. Tsai, Y. S. Choi, W. Ma, J. R. Pomeroy, C. Tang, and J. E. Ferrell, "Robust, tunable biological oscillations from interlinked positive and negative feedback loops," *Science*, vol. 321, no. 5885, pp. 126–129, 2008.
- [13] E. Marder, T. O'Leary, and S. Shrutli, "Neuromodulation of circuits with variable parameters: Single neurons and small circuits reveal principles of state-dependent and robust neuromodulation," *Annual Review of Neuroscience*, vol. 37, no. 1, pp. 329–346, 2014.
- [14] G. Drion, T. O'Leary, J. Dethier, A. Franci, and R. Sepulchre, "Neuronal behaviors: A control perspective," in *54th IEEE Conference on Decision and Control*, pp. 1923–1944, 2015.
- [15] R. Sepulchre, G. Drion, and A. Franci, "Control across scales by positive and negative feedback," *Annual Review of Control, Robotics, and Autonomous Systems*, vol. 2, pp. 89–113, 2019.
- [16] D. S. Bernstein, "Feedback control: an invisible thread in the history of technology," *IEEE Control Systems Magazine*, vol. 22, no. 2, pp. 53–68, 2002.
- [17] C. Chua, L.O a d Desoer and E. Kuh, *Linear and Nonlinear Circuits*. Mc Graw-Hill Book Company, 1987.
- [18] F. Forni and R. Sepulchre, "Differential dissipativity theory for dominance analysis," *IEEE Transactions on Automatic Control*, vol. 64, no. 6, pp. 2340–2351, 2018.
- [19] F. A. Miranda-Villatoro, F. Forni, and R. J. Sepulchre, "Analysis of lur'e dominant systems in the frequency domain," *Automatica*, vol. 98, pp. 76–85, 2018.
- [20] R. Smith, "Existence of period orbits of autonomous ordinary differential equations," in *Proceedings of the Royal Society of Edinburgh*, vol. 85A, pp. 153–172, 1980.
- [21] R. Smith, "Orbital stability for ordinary differential equations," *Journal of Differential Equations*, vol. 69, no. 2, pp. 265 – 287, 1987.
- [22] L. Sanchez, "Cones of rank 2 and the Poincaré–Bendixson property for a new class of monotone systems," *Journal of Differential Equations*, vol. 246, no. 5, pp. 1978 – 1990, 2009.
- [23] L. Sanchez, "Existence of periodic orbits for high-dimensional autonomous systems," *Journal of Mathematical Analysis and Applications*, vol. 363, no. 2, pp. 409 – 418, 2010.
- [24] W. Che and F. Forni, "A tunable mixed feedback oscillator," *arXiv preprint arXiv:2011.08564*, 2020. Available at <https://arxiv.org/abs/2011.08564>.
- [25] A. L. Hodgkin and A. F. Huxley, "A quantitative description of membrane current and its application to conduction and excitation in nerve," *The Journal of physiology*, vol. 117, no. 4, pp. 500–544, 1952.
- [26] A. Padoan, F. Forni, and R. Sepulchre, "The  $H_{\infty,p}$  norm as the differential  $L_{2,p}$  gain of a p-dominant system," in *Proceedings of the 58th IEEE Conference on Decision and Control*, 2019.
- [27] W. Che and F. Forni, "Shaping oscillations via mixed feedback," *arXiv preprint arXiv:2103.13790*. Submitted to *60th IEEE Conference on Decision and Control*, 2021.

## A. Proof of Theorem 4

For  $\lambda = 0$ , the problem is equivalent to the classic absolute stability problem. According to Theorem 2, the mixed feedback amplifier is 0-dominant if the Nyquist plot of the linear system  $G(s, k, \beta)$  lies to the right hand side of the line  $-1$  in the complex plane. Note that in the expression (5),  $G(s, k, \beta) = kG(s, 1, \beta)$ . Hence the condition on the Nyquist plot of  $G(s, k, \beta)$  is verified whenever  $0 \leq k < \bar{k}_0$ , by construction.

## B. Proof of Theorem 6

We will prove Theorem 6 by showing the shifted linear system  $G(s - \lambda, k, \beta)$  is 2-passive. The result will then follow from the interconnection theorem [18, Theorem 4].

The linear system  $G(s, k, \beta)$  is 2-passive if the shifted linear transfer function  $G(s - \lambda, k, \beta)$  is positive real, i.e.  $\angle G(s - \lambda, k, \beta) \in (-90^\circ, 90^\circ)$  for all  $s = j\omega$ , [19, Theorem 3.3]. For a linear system, a stable pole and an unstable zero can contribute to a  $90^\circ$  phase lag, while an unstable pole and a stable zero can contribute to a  $90^\circ$  phase lead. When  $\beta > \beta^*$ , the shifted linear system  $G(s - \lambda, k, \beta)$  has two unstable poles, one stable pole and one unstable zero.

**Case  $\tau_n < \tau_l$ :** as illustrated in Fig. 11, take  $\lambda = -\frac{p_p + p_n}{2}$ . As a consequence, the shifted linear system  $G(s - \lambda, k, \beta)$  has a stable pole and an unstable pole of the same magnitude, meaning that their contributions to the phase of the system cancel out. The shifted system then is left with a pair of unstable pole and zero, which guarantees the positive realness of  $G(s - \lambda, k, \beta)$ . This property holds for any  $k > 0$ , since  $k$  does not influence the positions of poles and zeros of the open loop transfer function.

**Case  $\tau_l < \tau_p$  and case  $\tau_p < \tau_l < \tau_n$ :** same as above, taking  $\lambda = -\frac{p_l + p_p}{2}$ .

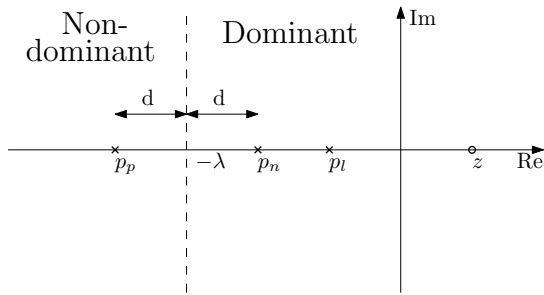


Fig. 11. Setting  $\lambda$  in the complex pole plane such that  $G(s - \lambda, k, \beta)$  is 2-passive

*Remark 2:* The rate  $\lambda$  does not necessarily need to locate exactly at the middle of the non-dominant and dominant poles, as in the proof. A small perturbation of  $\lambda$  from the middle position, for example, will introduce negligible fluctuations on the phase without violating the overall positive realness of  $G(s - \lambda, k, \beta)$ . The range of feasible  $\lambda$  will be wider for larger time-scale separation between dominant and non-dominant poles.

## C. Proof of Proposition 1

Note that  $C(s)$  in (12) is continuous along the real axis except at the poles. Then, for every  $\beta \in (0, 1)$  and for all  $i \in (1, 2, \dots, m - 1)$  and  $i \in (m + 1, m + 2, \dots, m + n - 1)$ ,

$$\begin{cases} \lim_{s \rightarrow -1/\tau_i^+} C(s) = \infty & \lim_{s \rightarrow -1/\tau_{i+1}^-} C(s) = -\infty \\ \lim_{s \rightarrow -1/\tau_i^+} C(s) = -\infty & \lim_{s \rightarrow -1/\tau_{i+1}^-} C(s) = \infty \end{cases} \quad (15)$$

Thus, for every  $\beta \in (0, 1)$ , by the intermediate value theorem  $C(z)$  must have at least one zero  $z \in (-1/\tau_i, -1/\tau_{i+1})$ , i.e. the zero  $z$  is in-between the poles of  $C_p(s)$  and  $C_n(s)$ . This continuity argument clarifies the relative position of  $m+n-2$  zeros with respect to the poles of  $C_p(s)$  and  $C_n(s)$ . Since  $C(s)$  can only have a total number of  $m+n-1$  zeros, we need to determine the relative position of one more zero.

We will show that the last zero must locate in the interval  $(-\infty, -1/\tau_1) \cup (-1/\tau_{m+n}, \infty)$ . If any, a zero  $z_0 \in (-\infty, -1/\tau_1) \cup (-1/\tau_{m+n}, \infty)$  guarantees that  $\frac{C_p(z_0)}{C_n(z_0)} > 0$ , i.e.  $C_p(z_0)$  and  $C_n(z_0)$  have the same sign and neither of them is equal to zero. It follows that any point in  $z_0 \in (-\infty, -1/\tau_1) \cup (-1/\tau_{m+n}, \infty)$  can be made a zero of  $C(s)$  by setting  $\beta = \frac{C_n(z_0)}{C_p(z_0) + C_n(z_0)} \in (0, 1)$ . Hence we have shown that for every  $z_0 \in (-\infty, -1/\tau_1) \cup (-1/\tau_{m+n}, \infty)$ , there is a  $\beta \in (0, 1)$  such that  $z_0$  is a zero of  $C(s)$ .

In summary, we have shown that  $C(s)$  has  $m+n-2$  zeros interlaced with poles from  $C_p(s)$  and  $C_n(s)$  and a zero  $z_0 \in (-\infty, -1/\tau_1) \cup (-1/\tau_{m+n}, \infty)$ , which already are  $m+n-1$  zeros. As final remark, we observe that there is a limit value of  $\beta$  for which the zero  $z_0$  moves towards infinity, given by

$$\beta = \lim_{z_0 \rightarrow \pm\infty} \frac{C_n(z_0)}{C_p(z_0) + C_n(z_0)}$$

For  $m = n = 1$ , this limit corresponds to  $\beta^*$  in Theorem 6.